Universitat Politècnica de Catalunya (UPC)
Universitat Autònoma de Barcelona (UAB)
Universitat de Barcelona (UB)
Institut de Ciències Fotòniques (ICFO)

http://www.photonicsbcn.eu

Master in Photonics

MASTER THESIS WORK

Quantum control of an ultracold quantum gas

Joan Agustí Bruzón

Supervised by Prof.Dr. Morgan Mitchell, (ICFO)

Presented on date 9th September 2019

Registered at

Escola Tècnica Superior d'Enginyeria de Telecomunicació de Barcelona

Quantum control of an ultracold quantum gas

Joan Agustí Bruzón

ICFO The Institute of Photonic Sciencies, Mediterranean Technology Park
Av. Carl Friedrich Gauss, 3, 009
Castelldefels (Barcelona), Spain

September 2019

E-mail: agusti2796@gmail.com

Abstract. This thesis is devoted to the study of quantum control of an ultracold atomic ensemble of ^{87}Rb. Stroboscopic probing is used to achieve real-time tracking of the collective spin magnitude and orientation via non-destructive Faraday probing. By means of an RF feedback scheme we achieve a reduction in angular dispersion of the precessing spin down to a circular standard deviation *circ std*(ϕ)=0.11(3) rad.

1. Introduction

Atomic Quantum Optics experiments rely on complex experimental setups and require precise control of their parameters. Real-time and high precision setting of the quantum state can be achieved via quantum feedback control. It relies on the steering of the quantum state towards the desired state by external state-dependent manipulation [1]. Quantum feedback control have been used to cool down an atomic spin ensemble [2], to generate macroscopic entangled states in a cold atomic ensembles [3], or to achieve quantum-noise reduction for quantum-enhanced sensing [4]. To measure the state and get a estimation of the parameters under study, most of this experiments use quantum non-demolition (QND) measurements due to its low disturbance on the system [5].

In this project we use stroboscopic probing of an ultracold atomic ensemble of ^{87}Rb to achieve real-time tracking of the precession angle and perform feedback on the atomic spin state via RF manipulation. Using this methods, we demonstrate a reduction in the angular dispersion of the precessing ensemble down to a mean value of circular standard deviation *circ std*(ϕ)=0.11(3) rad.

This work is organized as follows: Spin ensembles and the influence of external magnetic field are introduced in Sec. 2. The non-destructive Faraday probing technique is discussed in Sec. 3. Sec. 4 is devoted to radio frequency manipulation. The experimental setup and flow diagram for Faraday probing and real-time feedback are depicted in Sec. 5 and Sec. 6, respectively. The results are presented in Sec. 7. Finally, the conclusions and general outlook are given in Sec. 8.

2. Spin ensembles and Larmor precession

Consider an ensemble of ^{87}Rb atoms under a constant external magnetic field along the $\mathbf{z}$ direction, $\mathbf{B} = B_z\mathbf{z}$. Due to the action of the magnetic field, the energy levels of each hyperfine manifold are splitted, effect known as Zeeman splitting. Our case of study is the ground state manifold F=1 which consists of 3 energy sublevels, $m_F = \{1, 0, -1\}$. The spin of each atom can be mapped to the Bloch sphere, representing the spatial components $\hat{f}_x, \hat{f}_y$, and $\hat{f}_z$ of the total angular momentum $\hat{\mathbf{f}}$ [6] and thus, the collective spin of the ensemble of atoms is given by $\hat{F}_\alpha = \sum_{i=1}^{N_a} \hat{f}_\alpha^{(i)}$, where $\alpha \in (x, y, z)$ and N_a is the total number of atoms [7].

The interaction of the magnetic field and the atomic magnetic moment is described via

$$\hat{H}_0 = g_F \mu_B \mathbf{B} \cdot \hat{\mathbf{F}} = g_F \mu_B B_z \hat{F}_z, \tag{1}$$

where μ_B is the Bohr magneton and g_F is the Landé g-factor. Under this Hamiltonian, the spin dynamics corresponds to a rotation around the magnetic field at the Larmor frequency defined as $\omega_L = g_F \mu_B B_z/\hbar$ [7].

We define the expectation values of the angular momentum components as $F_i = \langle \hat{F}_i \rangle$ with $i \in (x, y, z)$ and the projection along the $\mathbf{y}$ axis of the total angular momentum is given by

$$F_y(t) = F_\perp \sin(\omega_L t), \tag{2}$$

where $F_\perp$ is the spin magnitude in the perpendicular plane.

The azimuthal angle of the spin is called the precession angle ϕ and is given by $\phi(t) = \int_0^t \omega_L(t')dt'$. We model the magnetic field experiences by the atoms as $B_z = \langle B_z \rangle + \delta B_z$ where $\langle B_z \rangle$ is a constant term representing the ensemble average over different experimental runs and δB_z is the contribution from shot-to-shot DC magnetic field fluctuations. For this type of fluctuations, the precession angle becomes:

$$\phi(t) = \omega_L t + \delta\omega_L t, \tag{3}$$

where $\delta\omega_L = \frac{g_F \mu_B}{\hbar}\delta B_z$. Therefore, as time goes on, the uncertainty in the magnetic field is a non negligible term and the precession angle ϕ becomes uncertain.

3. Faraday probing

Tracking the precession angle $\phi(t)$ is done by Faraday probing [8]. It relies on the Faraday rotation effect, where off-resonant linearly polarized light is rotated an angle θ by interacting with the atomic polarizability, described by the atom-light interaction Hamiltonian $\hat{H} = \hbar G_1 \tau_P^{-1} \hat{S}_z \hat{F}_y$ [7], where τ_P is the interaction time, $\hat{S}_z$ is the Stokes parameter, and G_1 is the vector atom-light coupling factor, see [8] for a explicit expression.

This rotation is proportional to the atomic spin projection along their propagation axis (the y-axis in our case) [9].

$$\theta(t) = G_1 F_y(t) = G_1 F_\perp \sin(\omega_L t), \tag{4}$$

where t is referenced to the start of the Faraday probing pulse.

Using a shot-noise limited differental photodetector (DPD) in balanced configuration, described in [10], the signal produced by the DPD is proportional to the Stokes parameter S_y, sensitive to the difference in number of photons in the ± 45 linearly polarized basis:

$$S_y = \frac{1}{2}(N_{+45^\circ} - N_{-45^\circ}) = \frac{N_L}{2}\left(\sin^2(45^\circ + \theta) - \cos^2(45^\circ + \theta)\right) \approx N_L \theta, \tag{5}$$

where N_{+45° and N_{-45° is the number of photons with linear $+45^\circ$ and linear -45° polarization, respectively, and N_L is the total number of photons. We have used that the DPD is in balanced configuration so $N_{+45^\circ} \approx N_{-45^\circ} \approx N_L/2$ and that the rotation polarization angle is small ($\sim$ mrad).

4. Radio frequency manipulation

In order to tilt the atomic spin direction, a radio frequency (RF) pulse perpendicular to the external magnetic field is sent to the ensemble. In our experiment, the external magnetic field goes along the **z** direction and the RF driving in the **y** direction.

The action of this pulse is described by an extended version of Eq. (1)

$$\hat{H} = \hbar\omega_L \hat{F}_z + 2\hbar\Omega \sin(\omega t + \varphi)\hat{F}_y = \hat{H}_0 + \hat{H}_1 \tag{6}$$

where the Rabi frequency has been defined as $\Omega = \frac{\mu_B g_F B_y}{2\hbar}$, ω and φ are the angular frequency and initial phase of the RF pulse, respectively.

It is convenient to describe the evolution in a rotating frame, i.e. in the interaction picture. In that case, the effective Hamiltonian is

$$\begin{aligned}\hat{H} = e^{i\hat{H}_0 t/\hbar}\hat{H}_1 e^{-i\hat{H}_0 t/\hbar} &= \hbar\Omega(\cos(\varphi)\hat{F}_y - \sin(\varphi)\hat{F}_z) \\ &= \hbar\Omega\hat{R}_z(\varphi)\hat{F}_y\hat{R}_z^\dagger(\varphi), \end{aligned} \tag{7}$$

where we have used the rotating wave approximation, assumed no detuning $\omega = \omega_L$, and used the rotation matrix $\hat{\mathbf{R}}_\mathbf{n}(\theta) = e^{-i\theta\mathbf{n}\cdot\hat{\mathbf{F}}}$.

The dynamics resulting from Eq.(7) are given by the time evolution operator $\hat{U}(t) = \exp\{(-iH(t)t/\hbar)\} = \exp\Big\{(-i\Omega t\hat{R}_z\hat{F}_y\hat{R}_z^\dagger)\Big\} = \hat{R}_{\vec{n}}(\Omega t)$ where $\vec{n} = (-\sin\varphi, \cos\varphi, 0)$. The net effect is a rotation around the axis set by $\vec{n}$ and by an angle Ωt. For example, for a rotation from the spin direction F_z to F_x, we need a RF pulse of $\Omega t = \pi/2$ and $\varphi = 0$.

5. Experimental setup

The experiments have been performed on a thermal cloud of ^{87}Rb. After 3.0s of all-optical evaporation in a crossed-beam optical dipole trap [9], a thermal cloud of about $N_a = 313(13) \times 10^3$ atoms and $T = 443(11)nK$ is achieved.

The probing and feedback scheme, see Figure 1, is an extension of earlier reported experimental setup [7]. Pulse generation and analysis are performed in real-time on a chipKIT uC32 microcontroller (PIC32). The microcontroller sends a gating pulse to the AOM generating sub-microsecond long light pulses which are linearly polarized and 280 MHz red detuned from the $1 \leftrightarrow 0'$ D_2 line transition of ^{87}Rb [11]. As precise timings are needed, the pulses are generated by interrupt routines on the microcontroller. Each interrupt routine generates the gating pulse. The core of the microcontroller runs at 80MHz, so the clock cycle (CLK cycle) period is 12,5ns. A differential photodetector takes the difference in signal that arrives from a polarizing beam splitter (PBS) which integrates and amplifies the signal before being forwarded to a Redpitaya development board (Zync 7010 SoC FPGA). The Redpitaya is programmed with two sample and hold modules (SHA and SHB) such that one is activated before the signal and the other just after. Then, the difference is taken and the result is sent to the microcontroller. This is repeated for each pulse. At the end of the sequence the interrupts routine stops and all data analysis is performed. When performing feedback control, the real-time information is used to compute the required initial phase adjustment of the RF waveform generator. For this purpose, the microcontroller generates a digital feedback signal which is wired to the trigger input port of the waveform generator. The device is connected to the RF coils of the experiment and is programmed to generate a custom RF pulse on a trigger

event. All parameters such as pulse length, pulse frequency, delays, etc. are set by a Python program, which interfaces the microcontroller over serial communication.

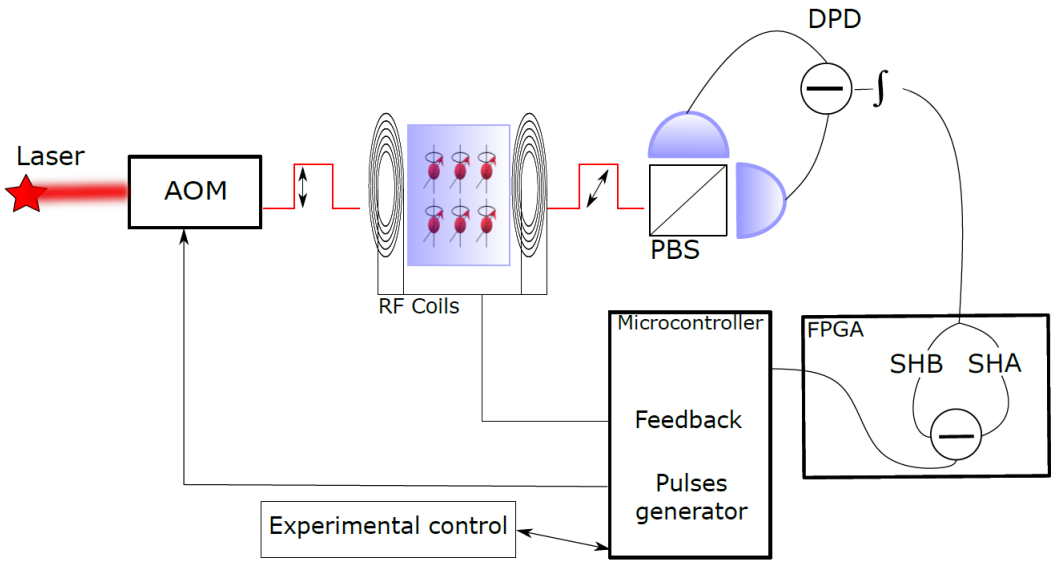

Figure 1: General setup for Faraday probing and real-time feedback. Atoms are precessing around an applied magnetic field B at Larmor frequency ω_L inside the chamber. A microcontroller triggers an acousto-optic modulator (AOM) to generate the desired length of the pulses at a repetition rate T_L. The pulses pass though a polarization beam splitter (PBS) placed before a differential photodetector (DPD) where they are integrated. The signal is analyzed by an FPGA that samples and holds the voltages before and after each pulse and computes their difference. The difference signal is read by a microcontroller which uses Fourier analysis to compute the precession angle ϕ. The feedback loop uses the obtained angle ϕ to adjust the initial phase of the RF waveform generator and trigger the RF pulse. All parameters are monitored via the main control system of the experiment.

6. Experimental sequence: real-time analysis and feedback

After the all optical evaporation, the experimental sequence starts with a $\pi/2$-RF pulse that tips the spins into the x-y plane (Figure 2a-2b). There, the external magnetic field of B=120 mG makes the spin precess at an angular frequency of $\omega_L = 2\pi \times 84$kHz (Figure 2c). This defines a Larmor period of $T_L = 11.9\mu s$. The microcontroller is programmed to send 3 pulses of $0.5\mu s$ to the ensemble at a repetition rate of $T_{rate} = 4/3T_L = 15.87\mu s$ (Figure 2d). We note that the optimal repetition rate would be at $1/3T_L = 3.97\mu s$, needed for a discrete Fourier analysis over one oscillation period. However, the timing constraints of the on-board analog-to-digital converter (ADC) required to increase the separation between Faraday pulses to $T_L + 1/3T_L = 4/3T_L$. The signal sampled by the microcontroller can be described by $s(t) = A\cos(\phi_i) + B\sin(\phi_i) + C$, where

the Fourier coefficients of the signal are described by $A = 2/3\sum_i^3 s_i \cos(\omega_L t_i)$, $B = 2/3\sum_i^3 s_i \sin(\omega_L t_i)$, and $C = 2/3\sum_i^3 s_i$, where $t_i = iT_L/3$, and $i \in \{0, 1, 2\}$ is the index labeling the 3 consecutive pulses. For the A and B coefficients, this reads:

$$A = \frac{2}{3}\left(s_0 \cos\left(0 \cdot \frac{2\pi}{3}\right) + s_1 \cos\left(1 \cdot \frac{2\pi}{3}\right) + s_2 \cos\left(2 \cdot \frac{2\pi}{3}\right)\right) \tag{8a}$$

$$B = \frac{2}{3}\left(s_0 \sin\left(0 \cdot \frac{2\pi}{3}\right) + s_1 \sin\left(1 \cdot \frac{2\pi}{3}\right) + s_2 \sin\left(2 \cdot \frac{2\pi}{3}\right)\right), \tag{8b}$$

then, the precession angle is ϕ=atan2(B,A). The provided implementation of the $atan2(B, A)$ function is time consuming, $\sim 75\mu s$, exceeding the requirements of this project. We circumvent this limitation by expanding to 3rd order the atan2 function in the regime $B/A = \pm 1$ using rotations in the A-B plane. The used expansion is [12] atan(x)$\approx (0.97239x) - (0.19195x^3)$ and reduces the implementation time to the range of 10.5 µs − 15.8 µs.

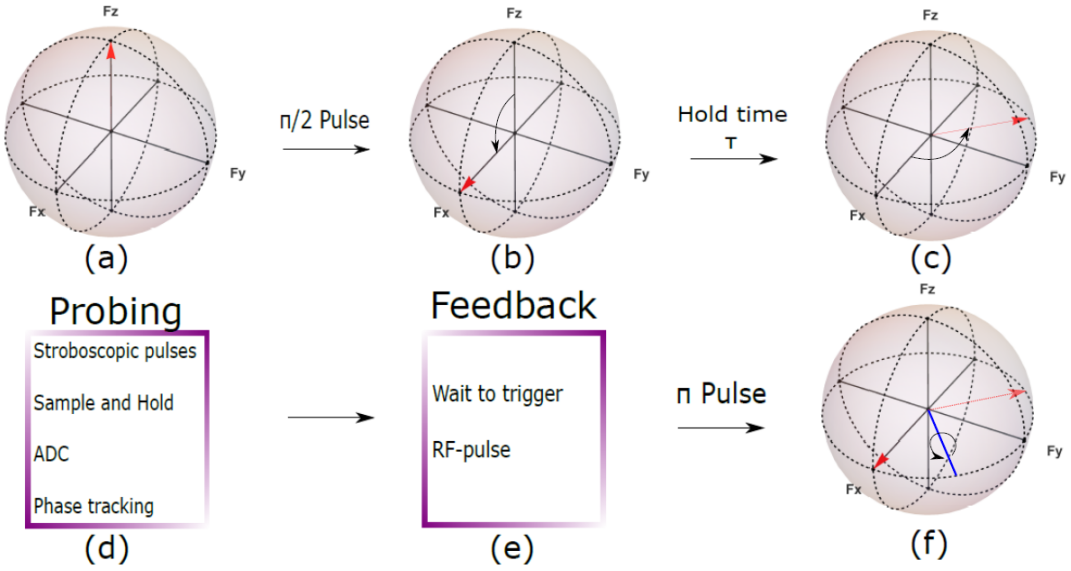

Figure 2: Flow diagram of the experimental realization. (a) The atomic ensemble starts with a magnetization along the external magnetic field. (b) A $\pi/2$-RF pulse is applied to rotate the axis to the perpendicular plane. (c) The spins start to precess around the magnetic field for a hold time τ. (d) We do stroboscopic probing consisting of pulse generation and readout of the Faraday signal via the FPGA and the microcontroller. (e) The feedback scheme adjust the initial phase of the RF waveform generator. It introduces a variable wait time before sending a trigger signal to the waveform generator. (f) The spin direction is rotated around the axis defined by half the precession angle (blue line) into a reference axis.

Hereafter, the system is allowed to freely evolve for a time $mod(-t_{meas} + \frac{\phi/2}{2\pi}T_L, T_L)$

where t_{meas} represents the total time comprising measurements and phase estimation (Figure 2e). Finally, the trigger signal is sent and a π-RF pulse is generated. Note that the previous hold time τ has provided the required dephasing between spin precession and RF signal such that the rotation axis has been adjusted to half way between the estimated spin orientation and the reference axis (Figure 2f).

7. Results

7.1. Real-time phase tracking

In this first subsection we test the quality of the real-time tracking of a thermal cloud of ^{87}Rb. As described in [7], the ensemble is initially prepared in the F=1 $m_F = -1$ state. Then a $\pi/2$-RF pulse tilts the spins direction to the perpendicular plane where they oscillate for a variable hold time τ. By increasing the hold time linearly we observe a linear increase in the estimated phase, as expected from $\Delta\phi = \omega_L \Delta\tau$.

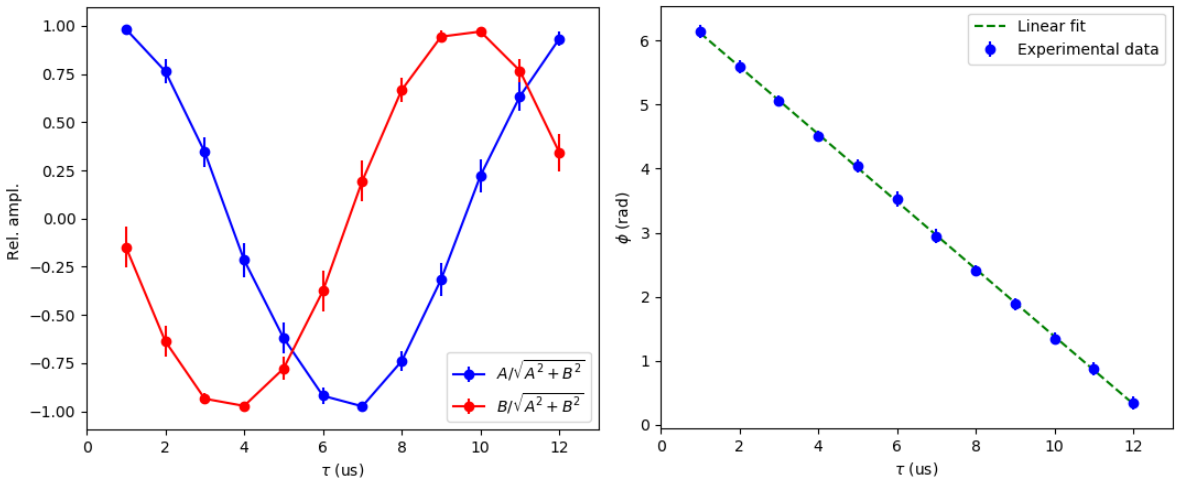

(a) (b)

Figure 3: Real-time tracking of (a) the relative Fourier coefficients given by Eq. (8*a*)-(8*b*) (b) the precession angle ϕ for different hold times τ. A linear model was fit to the data to acquire the slope, giving $\phi(\tau) = -0.52\tau + 6.64$ with a coefficient of determination $R^2 = 0.99991$.

In Figure 3(a) we show the oscillation of the measured Fourier coefficients A and B for different hold times τ. The corresponding evolution of the estimate precession angle ϕ is shown in Figure 3(b). Linear model accurately fits the experimental data, showing the expected slope in correspondence to the 84 kHz Zeeman splitting. The negative slope arises from the negative gyromagnetic ratio of the F=1 manifold in ^{87}Rb. These results verify the linearity in the phase estimation of our real-time tracking protocol.

7.2. Real-time feedback

This second subsection is devoted to the experimental results of the feedback scheme described in Sec. 6 (see Figure 2 for the logical sequence). The feedback scheme resets the precession angle of the precessing spins after different hold times τ and thus compensates for the effects of accumulated magnetic field noise. This magnetic field noise is caused by shot-to-shot fluctuations in the external magnetic field, arising from changes in the main power lines and operating electrical devices.

We use continuous Faraday probing (a light pulse of $40\mu s$) at the end of the sequence to estimate the precession angle w/ and w/o feedback (not depicted in Figure 2).

Without feedback, the magnetic noise is expected to lead to an uncertain spin orientation after a few miliseconds of precession [13].

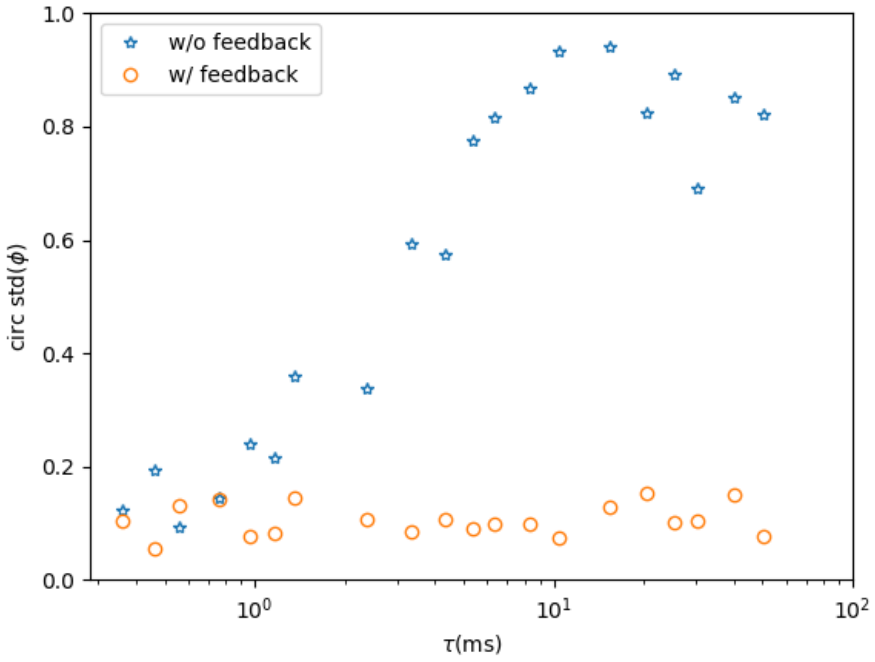

Figure 4: Circular standard deviation of the precession angle ϕ for different hole times τ. The blue stars show the dispersion without feedback. The green circles with feedback.

In Figure 4 the circular standard deviation (*circ std*) of the precession angle with and without feedback are presented. Without feedback we observe a rapid increase of the dispersion of ϕ. On the other hand, with feedback the dispersion of ϕ stabilizes to a mean value $circ\ std(\phi) = 0.11(3)$ rad.

For low hold times τ the precession angle ϕ has not yet accumulated enough magnetic field uncertainties so the dispersion is similar for with and without feedback.

8. Conclusion and outlook

We have presented results on real-time phase tracking and RF feedback in an ultracold ensemble of ^{87}Rb. The probing is based on stroboscopic pulses and give access to the spin amplitude and precession angle of ^{87}Rb in its ground state manifold. We used a linear model to fit the phase tracking for different hold times and verified a linear response with $R^2 = 0.99991$. The implemented feedback scheme compensates magnetic field uncertainties in the precession angle by rotating the spin state to a reference axis. By this we achieved a stable and reduced dispersion in the precession angle of *circ std*(ϕ)=0.11(3) rad. The here presented phase-tracking and feedback protocol can be applied for taking metrological advantage from interaction based spin squeezing.

Acknowledgements

I would like to acknowledge the people this project has given me the opportunity to work with: Morgan Mitchell, Chiara Mazzinghi, Sandhya Ganesh, Daniel Benedicto, and mostly, Pau Gómez. Moreover, I am grateful to the other group members without whom my time at ICFO would not have been the same.

References

[1] Serafini A 2012 *ISRN Optics* **2012**

[2] Behbood N, Colangelo G, Ciurana F M, Napolitano M, Sewell R and Mitchell M 2013 *Physical review letters* **111** 103601

[3] Behbood N, Ciurana F M, Colangelo G, Napolitano M, Tóth G, Sewell R and Mitchell M 2014 *Physical review letters* **113** 093601

[4] Inoue R, Namiki R, Sagawa T, Takahashi Y *et al.* 2013 *Physical review letters* **110** 163602

[5] Deutsch I H and Jessen P S 2010 *Optics Communications* **283** 681–694

[6] Kaminski F 2012 *Coherent Atom-Light Interaction in an Ultracold Atomic Gas Experimental Study of Faraday Rotation Imaging and Matter-Wave Superradiance* (Københavns Universitet. Niels Bohr Institutet)

[7] Álvarez S P 2017 *Single domain spinor bose-einstein condensate* Ph.D. thesis Universitat Politècnica de Catalunya (UPC)

[8] Koschorreck M 2010 *Generation of Spin Squeezing in an ensemble of Cold Rubidium 87* Ph.D. thesis

[9] Gomez P, Mazzinghi C, Martin F, Coop S, Palacios S and Mitchell M W

[10] Ciurana F M, Colangelo G, Sewell R J and Mitchell M W 2016 *Optics letters* **41** 2946–2949

[11] Steck D A 2001 Rubidium 87 d line data

[12] Tylor N 2017 How to find a fast floating-point atan2 approximation URL `https://www.dsprelated.com/showarticle/1052.php`

[13] Luan J 2017 *Closed-loop control of magnetic fields for atomic physics experiments* Master's thesis Universitat Politècnica de Catalunya